Photobiomodulation effects on active brain networks during a spatial memory task

Alba Gutiérrez-Menéndez , Sandra Cid-Duarte , María Banqueri , Juan A. Martínez , Marta Méndez , Jorge L. Arias

PII: S0031-9384(20)30605-3
DOI: https://doi.org/10.1016/j.physbeh.2020.113291
Reference: PHB 113291

To appear in: *Physiology & Behavior*

Received date: 2 October 2020
Revised date: 9 December 2020
Accepted date: 14 December 2020

Please cite this article as: Alba Gutiérrez-Menéndez , Sandra Cid-Duarte , María Banqueri , Juan A. Martínez , Marta Méndez , Jorge L. Arias , Photobiomodulation effects on active brain networks during a spatial memory task, *Physiology & Behavior* (2020), doi: https://doi.org/10.1016/j.physbeh.2020.113291

Photobiomodulation effects on active brain networks during a spatial memory task

Highlights

1. Photobiomodulation decreases CCO activity in many brain areas of control rats.
2. Both behavioural groups perform reversal memory task correctly.
3. Photobiomodulation decreases CCO levels in some brain areas involved in the task.
4. Photobiomodulation technique has more effects on active brain networks.

Photobiomodulation effects on active brain networks during a spatial memory task

Alba Gutiérrez-Menéndez*[ab], Sandra Cid-Duarte[a], María Banqueri[bc], Juan A. Martínez[bd], Marta Méndez[ab], Jorge L. Arias[ab].

[a] Laboratory of Neuroscience, Department of Psychology. University of Oviedo, Plaza Feijóo, s/n, E-33003, Oviedo, Spain.

[b] Instituto de Neurociencias del Principado de Asturias (INEUROPA), Oviedo, Spain.

[c] Molecular Neurobiology laboratory. Nencki Institute of Experimental Biology. Polish Academy of Sciences. Ludwika Pasteura 3, 02-093 Warsaw, Poland.

[d] Electronic Technology Area. University of Oviedo, 33204 Gijón, Spain.

*** Corresponding author:** Laboratory of Neuroscience, Department of Psychology. University of Oviedo, Plaza Feijóo, s/n, E-33003, Oviedo, Spain. E-mail: Phone number:

Abstract

Photobiomodulation (PBM) or the use of red to near-infrared irradiation spectrum, is a non-invasive intervention that produces neurostimulatory effects and reaches benefits in several pathologies as well as in healthy subjects. The main objective of this study was to evaluate and compare the effects of PBM in a rat brain network on basal state and functional activity during the execution of a reversal task. Twenty-eight rats were divided into four groups: control group (*n*=7), control photobiomodulation group (*n*=8), behavioural group (*n*=6) and behavioural photobiomodulation group (*n*=7). Reversal memory was assessed using a Morris water maze and cytochrome c oxidase (CCO) was used as a brain metabolic activity marker. After five days of PBM, the control photobiomodulation group showed a decrease of CCO levels in the striatum, medial septum, entorhinal, hippocampus, amygdala, thalamus, mammillary nuclei and VTA. Both behavioural groups performed the task correctly, however, the behavioural photobiomodulation group displayed CCO reduction in some regions involved in the execution of the reversal task: septum, entorhinal, CA1, CA3, central amygdala and supramammilar, along

with higher levels in accumbens. These results could show the effect of PBM on active brain networks. Further studies will be necessary to elucidate its effects in different brain networks that are involved in the execution of other memory tasks.

Keywords: photobiomodulation, near-infrared light, spatial memory, brain networks, cytochrome c oxidase.

Abbreviations: AccC, Accumbens Core; AccSh, Accumbens Shell; AD, Thalamus anterodorsal; AM, Thalamus anteromedial; ATP, adenosine triphosphate; AV, Thalamus anteroventral; BC, behavioural control group; BC+PBM, behavioural photobiomodulation control group; BLA, Basolateral Amygdala; C, control group; CCO, cytochrome c oxidase; CeA, Central Amygdala; CG, Cingulate cortex; C+ PBM, control photobiomodulation group; DG, Dentate Gyrus; ENT, Entorrinal cortex; IL, Infralimbic cortex; LaA, Lateral Amygdala; LS, Lateral Septum; MML, Medial Lateral Mammillary; MMM, Medial Medial Mammillary; MS, Medial Septum; MWM, Morris water maze; PBM, photobiomodulation; PL, Prelimbic cortex; PRh, Perirhinal cortex; ROS, reactive oxygen species; STD, Dorsal Striatum; SuM, Supramammilar; VTA, Ventral Tegmental Area.

1. Introduction

Currently, photobiomodulation (PBM) is one of the most promising therapies based on the use of red to near-infrared irradiation spectrum (600-1100 nm) [1]. This non-invasive intervention produces neurostimulatory effects and reaches numerous beneficial results in a significant number of varied fields [2]. Thus, it is widely used to treat inflammatory conditions, pain, wound healing of deep and superficial tissues and even for aesthetic purposes and welfare [3,4]. Similarly, PBM has been proven effective in dentistry, dermatology and as well as clinical pathologies such as traumatic brain injuries, neurodegenerative diseases, cancer, tumours and in several psychiatric disorders [5–8]. Thus, PBM could become one of the most significant light therapies in the near future [9].

The action mechanism of this therapy is the absorption of the light by the mitochondria, specifically by the enzyme cytochrome c oxidase complex (CCO), the terminal enzyme in the

respiratory electron transport chain. This absorption has a large range of significant effects being the improvement of metabolic function and the increase of adenosine triphosphate (ATP) synthesis the most supported mechanisms of action [10]. Furthermore, it has been found that PBM increases DNA synthesis, intracellular calcium, Delta CCO and oxygenated haemoglobin concentrations and it activates many signalling pathways, such as the anti-apoptotic and pro-survival signalling [3,6,10]. PBM also leads to a dissociation of nitric oxygen species that follows the generation of reactive oxygen species (ROS) resulting in greater oxidation and the activation of many transcription factors causing long-lasting cell effects [3,11]. In addition, this technique can regulate the immune system response and stimulate neurogenesis, synaptogenesis and neuroplasticity [6,12]. However, some studies have also described some adverse effects induced by the use of PBM such as the increase of oxidative stress and the damage of DNA, the existence of apoptosis in an hippocampal cell culture, a delay on brain repair on traumatic injury in the mouse brain and increased diastolic pressure in major depression [13–16].

The assessment of the CCO activity in numerous studies has shown that the brain energy demand involved in neuronal activity during a specific behavioural task is increased in the brain areas that are involved in the task execution and, also, this brain activity is related to the difficulty of task performance [17–20]. Conversely, it has been found that after a learning process in a behavioural task, there is a reduction in CCO activity, therefore increasing the efficiency of the region's activity in regard to metabolic costs [21]. Thus, Olson et al. [22] showed a correlation between a decrease in blood flow and the improvement of the performance in a serial response time task and, Gobel et al. [23] found a pattern of deactivation in several areas, improving the efficiency of the visuomotor processing in the Serial Interception Sequence Learning task. In the same way, El Khoury et al. [24] using PBM to examine its effects in normal subjects after two different tasks, found an activity reduction in several brain areas involved in one of the tasks. Consequently, they suggested that near-infrared light had significant effects on brain activity but only when the brain region is functionally active executing an specific task and, this activity reduction could be a light protective effect [24].

Taking into account these potential benefits reached by PBM during a task and its effects on the CCO activity, the use of this therapy could have a differential effect on the brain networks if the areas are functionally active and these effects could be positive, prompting an enhanced efficiency of the metabolic process. Our study aimed to assess and compare the metabolic effects of PBM in a basal state network and in a functionally active neural brain network during the execution of a spatial reversal memory test. This behavioural protocol entails the ability to flexibly shift response patterns after a change in environmental conditions [25], a process that is mainly mediated by the prefrontal cortex [26]. Reversal memory is mostly impaired in several pathologies such as attention deficit hyperactivity disorder, autism, schizophrenia, Alzheimer's disease, and Parkinson's disease [27,28]. It therefore becomes crucial to determinate if PBM could be a potential treatment that could modulate brain activity underlying this cognitive function. Thus, rats of the behavioural groups performed a reversal memory test in the Morris water maze (MWM) and then, both experimental groups, one that performed the task and another without learning, received PBM just behind the eyes to target mostly frontal areas. Brain function was compared with control conditions studying brain metabolic activity of the areas involved in the task by means of CCO histochemistry.

2. Materials and Method

2.1 Subjects

A total of 28 3-month-old male Wistar rats were used. All the animals were maintained at constant room temperature (22 ± 2 °C), with a relative humidity of 65–70% with an artificial light-dark cycle of 12 h (8:00–20:00/20:00–8:00) and *ad libitum* access to food and tap water. The procedures and manipulation of the animals were carried out according to European Communities Council Directive 2010/63/ EU and Royal decree N° 53/2013 of the Ministry of the Presidency related to the protection of animals used for experimentation and other scientific purposes. The local committee for animal studies of the Oviedo University approved the study.

Animals were randomly distributed into four groups: control group (C, *n*=7), control photobiomodulation group (C+PBM, *n*=8), behavioural control group (BC, *n*=6) and behavioural photobiomodulation control group (BC+PBM, *n*=7). We carried out two different experiments in order to assess the metabolic effects of photobiomodulation therapy. In experiment 1, we compared C and C+PBM groups to assess the effects of PBM on basal control rats and, in experiment 2 we evaluated its effects on animals subjected to behavioural procedures, comparing results of BC and BC+PBM groups.

2.2. Reversal task in the Morris water maze

Animals of BC and BC+PBM groups were trained in the MWM, a circular pool of 150 cm diameter placed in the centre of a 16 m^2 lit room (two lamps of 4000 lx) surrounded by black panels on which different spatial cues were placed. The water level was 30 cm, at a temperature of 22 ± 2 °C. The scape platform used was a cylinder, 10 cm in diameter, placed 2 cm below the water. The pool was divided into four equal imaginary quadrants (A, B, C and D) to locate start positions and platforms. The behaviour of the animal in the MWM was recorded using a video camera (Sony V88E) connected to a computer with the software EthoVision Pro (Noldus Information Technologies, Wageningen, the Netherlands).

Behavioural procedures carried out were described in Banqueri et al. [29] and the learning protocol consisted of six days. The first day was devoted to the habituation of the animals to the task in which the animals carried out four trials with a visible platform situated in the centre of the pool. On the following four days, animals were training with a reference memory test where they received four acquisition trials per training session or day, in which the platform was hidden in the centre of quadrant D. Each animal was placed in the water in one pseudo-randomized quadrant and then, given 60 seconds to find the platform. If the rat did not reach the platform after this time, it was placed on the platform for 15 seconds. During the inter-trial interval, they were placed in a black bucket for 30 seconds. Daily, at the end of the session, a 25-second transfer learning trial was performed, where the platform was removed to measure the percentage of time spent in each quadrant.

On the last day, the sixth day, reversal learning was tested. The rats carried out eight acquisition trials where the scape hidden platform was moved to the quadrant opposite to its previous location, quadrant C. Experimental conditions were the same as in the memory training. Escape latencies and the time of permanence in each quadrant were recorded during the acquisition.

2.3. Photobiomodulation Therapy

The photobiomodulation therapy performed was described in Banqueri et al. [29]. Animals of C+PBM and BC+PBM groups were housed in individual cages and received photobiomodulation for five days coinciding with the habituation day and the four days of the reference memory test. Three days before therapy, animals were habituated to photobiomodulation. In this habituation, we attached Velcro to their previously shaved heads, on the first third of the head just behind the eyes, in attempts to target mostly frontal areas. During the following five days, the animals received 60 cycles (20 seconds ON and 40 seconds OFF) with a total duration of one hour, daily, using a wavelength of 1,064nm with an applied power of 30mW. Approximately 1.1% of the applied power reaches the brain tissue and the applied dose was 20J/cm^2.

2.4. Cytochrome oxidase histochemistry

Ninety minutes after the end of the reversal task, the animals were decapitated. Brains were removed, frozen rapidly in N-methyl butane (Sigma-Aldrich, Madrid, Spain), and stored at -40ºC. The protocol carried out for the tissue treatment was described by Banqueri et al. [29]. Coronal sections (30 μm) of the brain were cut at -22 ºC in a cryostat (Leica CM1900, Germany). To quantify enzymatic activity and control staining variability across different baths, sets of tissue homogenate standards from the Wistar rats' brains were cut at different thicknesses (10, 30, 50 and 70 μm) and included with each bath of slides.

Sections and standards were fixed for 5 min in 0.1 M phosphate buffer with 10% (w/v) sucrose and 25% glutaraldehyde, pH 7.6. Next, baths of 0.1M phosphate buffer with 10% (w/v) sucrose were given for 5 min each, and one bath of 0.05M Tris buffer, pH 7.6 (0.275 mg/l

cobalt chloride (Aldrich, Germany), 10% (w/v) sucrose (Sigma, Germany), 6 g/l Trizmabase (Sigma, USA), and 0.5% (v/v) dimethyl-sulfoxide (Sigma-Aldrich, Madrid, Spain) for 10 min. Then, they were maintained in 0.1M phosphate buffer, pH 7.6, for 5 min and incubated in a solution of 0.0075% (w/v) cytochrome c oxidase (Sigma-Aldrich, Madrid, Spain); 0.002% (w/v) catalase (Sigma, Spain); 5% (w/v) sucrose (Sigma, Germany); 0.25% (v/v) dimethyl-sulfoxide (Sigma- Aldrich, Madrid, Spain); and 0.05% (w/v) diaminobenzidine tetra-hydrochloride (Sigma-Aldrich, Madrid, Spain) in 800 ml of 0.1M phosphate buffer at 37 °C for 1 h. Subsequently, the reaction was stopped by fixing the tissue in buffered 4% (v/v) formalin. Finally, sections were dehydrated, cleared with xylene (Avanter, Poland), and cover-slipped with Entellan (Merck, Germany).

2.5. CCO optical density quantification

The densitometric quantification of CCO activity was carried out by means of analysing the images of the regions of interest of the brain using a high precision illuminator, a digital camera and a computer equipped with the MCID Core 7.0 program (MCID, Interfocus Imaging Ltd., Linton, England). The mean optical density of each region was measured using three consecutive sections from each subject. In each section, four non- overlapping readings were taken, using a square-shaped sampling window adjusted for each region size. These measurements were averaged to obtain one mean per region for each subject. Then, optical density values were converted to CCO activity units, determined by the enzymatic activity of the standards measured spectrophotometrically [30].

The regions of interest were defined according to the stereotactic atlas of Paxinos and Watson [31], and the distance in mm of the regions counted from bregma was the following: +3.20mm for the cingulate (CG), prelimbic (PL) and infralimbic (IL) cortices; +1.56 mm for the dorsal striatum (STD) and the ventral striatum (Accumbens Core; AccC, Accumbens Shell; AccSh), +1.92 for septum (medial; MS and lateral; ML); -1.20 for the anterodorsal, anteromedial and anteroventral thalamus (AD, AM, AV); -2.28 mm for the CA1, CA3, and dentate gyrus (DG) subfields of the dorsal hippocampus, perirhinal cortex (PRh) and amygdala

(Basolateral; BLA, Central; CeA, Lateral; LaA) and -4.56 mm for the supramammillary (SuM), medial medial mammillary (MMM), medial lateral mammillary (MML), ventral tegmental area (VTA) and entorhinal cortex (ENT) (Fig. 1).

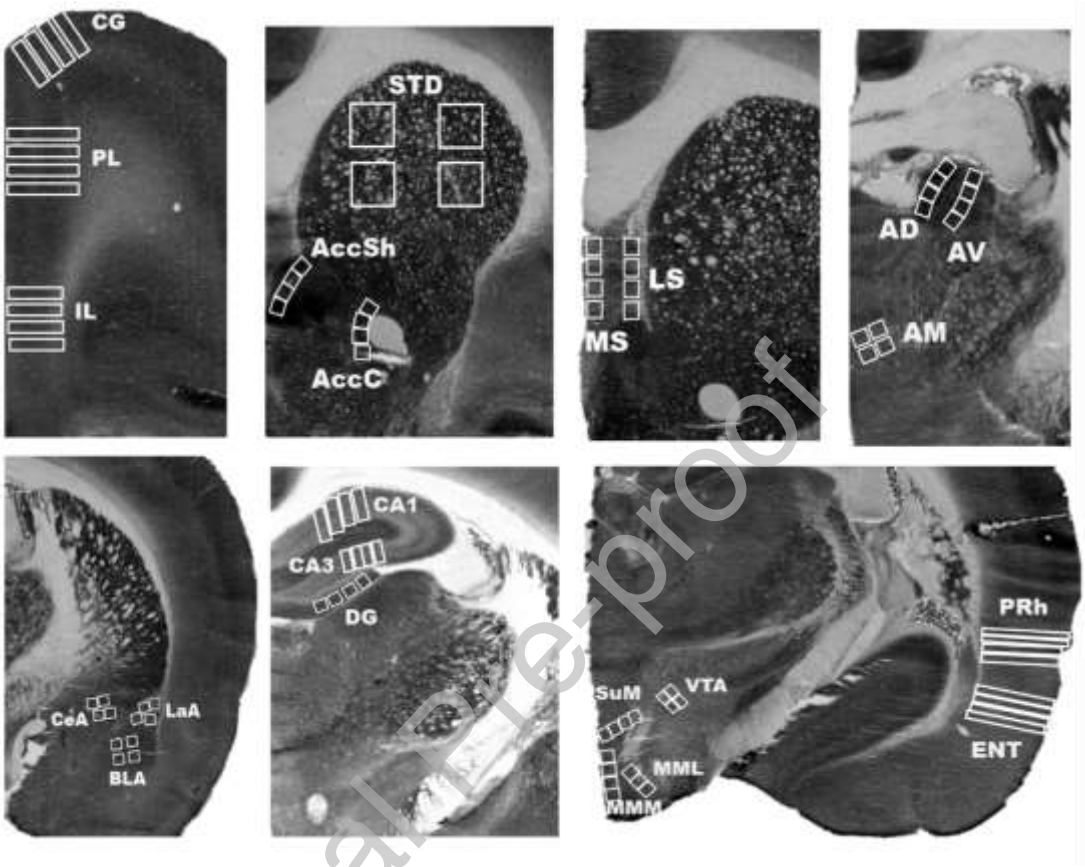

Fig. 1. Regions of interest. Sampling frames of CCO histochemistry in the brain regions of interest. Cingulate cortex= CG, Prelimbic cortex=PL, Infralimbic cortex=IL, Dorsal Striatum=STD, Accumbens Shell=AccSh, Accumbens Core=AccC, Medial Septum=MS, Lateral Septum= LS, Thalamus anterodorsal=AD, Thalamus anteromedial=AM, Thalamus anteroventral=AV, Basolateral Amygdala=BLA, Central Amygdala=CeA, Lateral Amygdala=LaA, field CA1 of hippocampus=CA1, field CA3 of hippocampus=CA3, Dentate Gyrus=DG, Supramammilar=SuM, Medial Medial Mammillary=MMM, Medial Lateral Mammillary=MML, Ventral Tegmental Area=VTA, Perirhinal cortex=PRh, Entorrinal cortex=ENT.

2.6. Statistical analysis

The data obtained was analysed using the software Sigma-Stat 12.5 (Systat Software Inc., Richmond, California). The significance level was defined as $p < 0.05$. Graphic representation of the results was performed with the SigmaPlot 12.5 software (SPSS Inc. and IBM Company, USA). All data was expressed as mean ± SEM.

Regarding behavioural data, escape latencies were analysed separately for each group and day using a one-way repeated-measures ANOVA. Post hoc comparisons were done when significant differences were found using Tukey test. The time spent in each quadrant (A, B, C, D) was analysed using one *t*-test per group and day comparing the target quadrant permanence (D in reference memory training and C during reversal memory training) with the other three quadrants. A non-parametric Mann-Whitney U-test was performed when the normality test failed.

Statistical comparisons of CCO activity values in each brain region were analysed using a *t*-test. Mann-Whitney U test was applied when the normality assumption failed. Group differences CCO activity in each brain region of interest were analysed using one-way ANOVAs, following by post hoc comparisons using the Holm-Sidak method. Kruskal-Wallis One-Way Analysis of Variance o Ranks (H) was performed when equal variance failed, and Dunn's Method was used as a multiple comparison procedure.

3. Results

3.1. Behavioural results of BC and BC+PBM groups

Analysis of the escape latencies during reference memory training did not show a main effect of day in BC group ($F_{3,15}$=1.479, p=0.260). Nevertheless, BC+PBM group showed statistically significant differences throughout the days ($F_{3,18}$=5.655, p=0.007), but only between the first and fourth training day (p = 0.004) (Fig. 2A).

In regards to the time spent in the quadrants, BC group spent more time in the target quadrant (D) during the probe trials of the reference memory training (D1: $t_{(22)}$ = -4.872, p<0.001; D2: $t_{(22)}$ = -4.625, p<0.001; D3: $t_{(22)}$ = -2.111, p= 0.046; D4: $t_{(22)}$ = -3.394, p= 0.003). The analysis of the probe trial of the reversal memory training data of day 5 showed preserved cognitive flexibility, with preference to the new reinforced quadrant (C) over the others (D5: $t_{(22)}$ = -2.250, p<0.035) (Fig. 2B). Similarly, BC+PBM group showed a preference for the rewarded quadrant (D) during all days of reference memory training (D1: U=27.000, n_1= 7, n_2= 21, p= 0.015; D2:

$t_{(26)}$ = -3.721, p<0.001; D3: $t_{(26)}$ = -3.989, p< 0.001; D4: $t_{(26)}$ = -4.738, p<0.001) and also more permanence in the target quadrant (C) during reversal memory training (D5: $t_{(26)}$ = -2.211, p= 0.036), exhibiting cognitive flexibility (Fig. 2C).

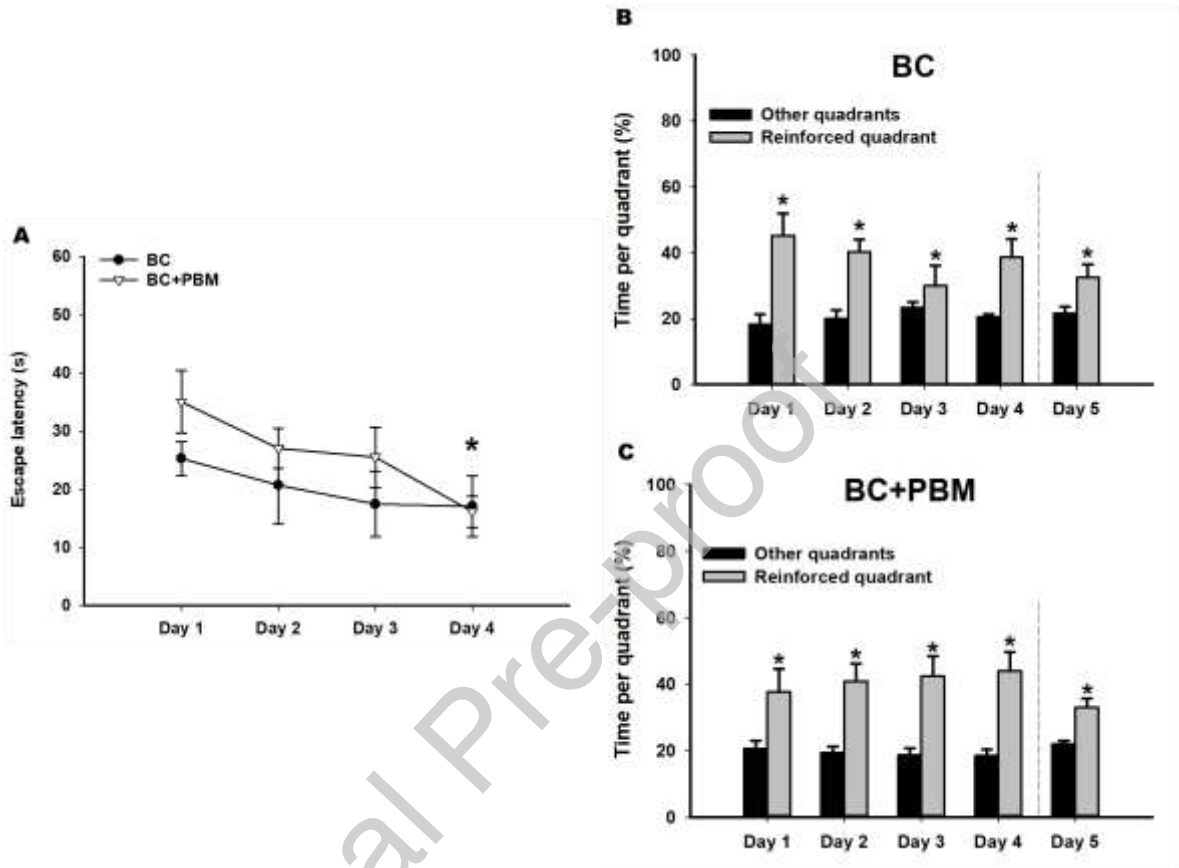

Fig. 2. Morris water maze behavioural results (Mean ± SEM). **A.** Escape latencies of BC and BC+PBM groups. The *x*-axis shows the days. Only BC+PBM group showed a decrease in escape latency on the fourth day (* p<0.05). **B.** Permanence of BC group in each quadrant (A, B, C, D) during the probe trials. BC subjects reached the learning criteria on the first day and showed intact cognitive flexibility (* p<0.05). **C.** Permanence of BC+PBM group in each quadrant (A, B, C, D) during the probe trials. This group also reached the learning criteria on the first day and showed intact cognitive flexibility (* p<0.05). The *x*-axis shows the days. Grey bars show percentage of permanence in reinforced quadrant (D during reference memory training and C, on day 5, during reversal memory training). Black bars represent the average permanence in the rest of the quadrants. Behavioural control group=BC, Behavioural photobiomodulation control group=BC+PBM.

3.2. CCO activity

In experiment 1, analysing the differences on CCO activity between C and C+PBM group, we found that PBM treatment reduced CCO units in dorsal and ventral striatum (STD: $t_{(13)}$ = 3.684, p=0.003; AccC: $t_{(13)}$ = 2.857, p=0.013; AccSh: U=9.000, n_1= 7, n_2= 8, p= 0.029), MS ($t_{(13)}$ = 6.962, p<0.001), ENT ($t_{(12)}$ = 3.513, p=0.004), hippocampus (CA1: $t_{(13)}$ = 3.294, p=0.006; CA3: $t_{(13)}$ = 3.727, p=0.003; DG: $t_{(13)}$ = 3.034, p=0.010), amygdala

(CeA: $t_{(12)}$ = 7.706, p<0.001; LaA: U=4.000, n_1= 7, n_2= 7, p= 0.007; BLA: U=1.000, n_1= 7, n_2= 7, p= 0.001), thalamus (AD: $t_{(13)}$ = 2.346, p=0.035; AV: $t_{(13)}$ = 2.969, p=0.011; AM: $t_{(13)}$ = 2.686, p=0.019), mammillary nuclei (MMM: $t_{(10)}$ = 3.112, p=0.011; MML: U=4.000, n_1= 6, n_2=6, p= 0.026; SuM: U=0.000, n_1= 6, n_2=6, p= 0.002) and ATV ($t_{(10)}$ = 3.341, p=0.007) (Fig. 3A)

Likewise, in experiment 2, BC+PBM group showed fewer CCO units than BC group in MS ($t_{(11)}$ = 3.262, p=0.008), ENT ($t_{(11)}$ = 2.438, p=0.033), CA1 ($t_{(10)}$ = 3.569, p=0.005), CA3 ($t_{(10)}$ = 3.314, p=0.008), CeA ($t_{(11)}$ = 2.256, p=0.045), and SuM ($t_{(10)}$ = 2.390, p=0.038), but not in AccC (U=6.000, n_1= 6, n_2= 7, p= 0.035), where BC+PBM group had higher CCO units (Fig. 3B).

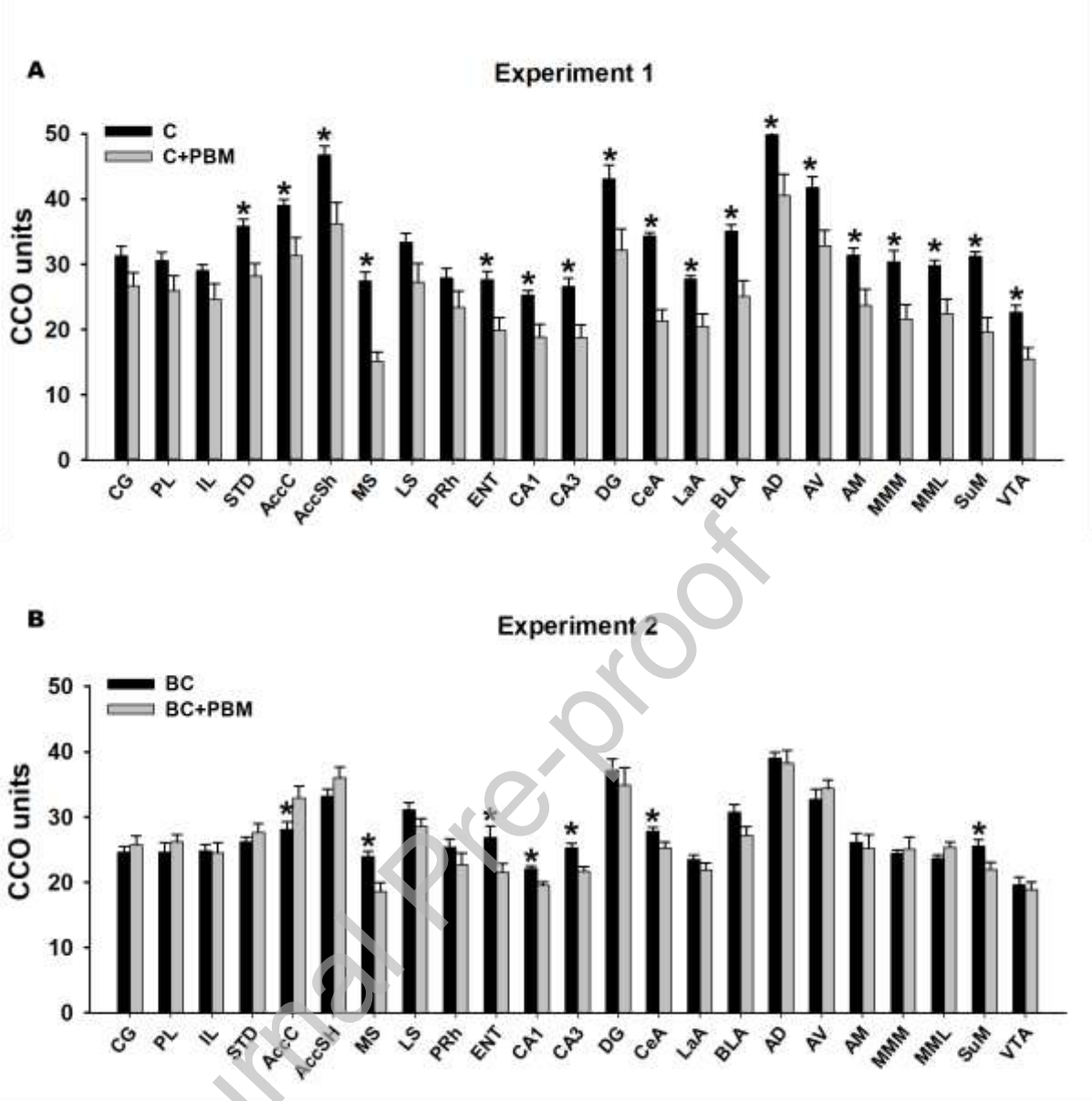

Fig. 3. CCO results (mean + SEM). **A.** CCO values in C and C+PBM groups. There were significant differences between the groups in STD, AccC, AccSh, MS, ENT, CA1, CA3, DG, CeA, LaA, BLA, AD, AV, AM, MMM, MML, SuM and VTA (*p<0.05). **B.** CCO values in BC and BC+PBM groups. Significant differences were found in AccC. MS, ENT, CA1, CA3, CeA and SuM (*p<0.05). Groups: control group=C, Control photobiomodulation group = C+PBM, Behavioural control group = BC, Behavioural photobiomodulation control group=BC+PBM. Areas: Cingulate cortex= CG, Prelimbic cortex=PL, Infralimbic cortex=IL, Dorsal Striatum=STD, Accumbens Shell=AccSh, Accumbens Core=AccC, Medial Septum=MS, Lateral Septum= LS, Thalamus anterodorsal=AD, Thalamus anteromedial=AM, Thalamus anteroventral=AV, Basolateral Amygdala=BLA, Central Amygdala=CeA, Lateral Amygdala=LaA, field CA1 of hippocampus=CA1, field CA3 of hippocampus=CA3, Dentate Gyrus=DG, Supramammilar=SuM, Medial Medial Mammillary=MMM, Medial Lateral Mammillary=MML, Ventral Tegmental Area=VTA, Perirhinal cortex=PRh, Entorrinal cortex=ENT.

Finally, CCO units of C, BC and BC+PBM groups were contrasted to analyse more deeply the potential differences in their metabolic activity. Significant group differences in CCO activity were found in the prefrontal cortex (CG: $F_{2,16}$=7.768, p=0.004; PL: $F_{2,16}$=5.857, p=0.012; IL: $F_{2,16}$=4.715, p=0.025), dorsal and ventral striatum (STD: $F_{2,17}$=22.243, p<0.001; AccC: H_2=12.247, p=0.002; AccSh: H_2=12.121, p=0.002), septum (MS: $F_{2,17}$=14.117, p<0.001;

LS: $F_{2,17}$=3.957, p=0.039), ENT ($F_{2,17}$=5.355, p=0.016), hippocampus (CA1: $F_{2,16}$=22.485, p<0.001; CA3: $F_{2,16}$=6.491, p<0.009; DG: $F_{2,16}$=3.860, p=0.043), amygdala (BLA: $F_{2,17}$=12.291, p<0.001; CeA: $F_{2,17}$=46.678, p<0.001; LaA: H_2=13.566, p=0.001), thalamus (AD: $F_{2,17}$=14.000, p<0.001; AM: H_2=7.898, p=0.019; AV: $F_{2,17}$=9.999, p=0.001) and in mammillary nuclei (SuM: $F_{2,15}$=23.280, p<0.001; MMM: $F_{2,15}$=4.753, p=0.025; MML: $F_{2,15}$=18.808, p<0.001) but not in PRh ($F_{2,17}$=2.957, p=0.079) and VTA ($F_{2,15}$=2.972, p=0.082). The statistical analysis of pair-wise differences between groups using the Holm-Sidak method showed an overall pattern of CCO activity increase in C group as compared to BC group in prefrontal cortex (CG: t= 3.635, p=0.007, PL: t= 3.296, p=0.014, IL: t= 2.533, p=0.044), dorsal and ventral striatum (STD: t= 6.066, p<0.001, AccC: Q= 3.494, p<0.05, AccSh: Q= 3.313, p<0.05), CA1 (t= 3.732, p=0.004), amygdala (BLA: t= 2.612, p=0.036; CeA: t= 6.496, p<0.001; LaA: Q= 2.633, p<0.05), AD (t= 4.280, p=0.001), AV (t= 4.123, p=0.002) and in mammillary nuclei (SuM: t= 4.161, p=0.002; MMM: t= 2.822, p=0.038; MML: t= 5.936, p<0.001).

In addition, C group showed greater CCO activity than BC+PBM group in CG (t= 3.030, p=0.016), IL (t= 2.709, p=0.046), STD (t= 5.346, p<0.001), AccSh (Q= 2.530, p<0.05), septum (MS: t= 5.278, p<0.001; LS: t= 2.812, p=0.036), ENT (t= 3.018, p=0.023), hippocampus (CA1: t= 6.665, p<0.001; CA3: t= 3.521, p=0.008; DG: t= 2.666, p=0.050), amygdala (BLA: t= 4.951, p<0.001; CeA: t= 9.394, p<0.001; LaA: Q= 3.524, p<0.05), thalamus (AD: t= 4.785, p<0.001; AM: Q= 2.711, p<0.05; AV t= 3.499, p=0.005) and in mammillary nuclei (SuM: t= 6.764, p<0.001; MMM: t= 2.487, p=0.050; MML: t= 4.304, p=0.001).

Also, BC group showed higher CCO activity than BC+PBM group in MS (t= 3.075, p=0.014), ENT (t= 2.560, p=0.040), CA1 (t= 2.826, p=0.012), CA3 (t= 2.481, p=0.049), BLA (t= 2.144, p=0.047), CeA (t= 2.529, p=0.022), SuM (t= 2.603, p=0.020) (Table 1).

Table 1. Cytochrome oxidase activity of the selected brain regions in the studied groups (means and S.E.M.)

Regions	C	BC	BC+PBM
Prefrontal cortex			
Cingulate cortex	31,31 ± 1,48	* 24,62 ± 0,87	# 25,73 ± 1,43
Prelimbic cortex	30,57 ± 1,27	* 24,65 ± 1,44	26,21 ± 1,14
Infralimbic cortex	29,01 ± 0,95	* 24,80 ± 1,03	# 24,50 ± 1,57
Dorsal Striatum	35,84 ± 1,06	* 26,20 ± 0,74	# 27,68 ± 1,34
Ventral Striatum			
Accumbens Core	39,02 ± 0,89	* 28,14 ± 1,12	32,93 ± 1,84
Accumbens Shell	46,80 ±1,31	* 33,19 ± 1,12	# 36,01 ± 1,65
Septum			
Medial septum	27,49 ± 1,31	23,99 ± 0,78	& # 18,58 ± 1,37
Lateral septum	33,39 ± 1,37	31,11 ± 1,07	# 28,61 ± 1,18
Perirhinal	27,87 ± 1,51	25,39 ± 1,23	22,73 ± 1,73
Entorhinal	27,63 ± 1,29	26,92 ± 1,75	& # 21,52 ± 1,40
Hippocampus			
CA1	25,23 ± 0,74	* 22,04 ± 0,48	& # 19,53 ± 0,52
CA3	26,57 ± 1,25	25,24 ± 0,79	& # 21,64 ± 0,75
Dentate gyrus	43,11 ± 2,05	37,17 ± 1,76	# 34,89 ± 2,73
Amygdala complex			
Basolateral n.	35,12 ± 0,94	* 30,76 ± 1,15	& # 27,19 ± 1,34
Central n.	34,32 ± 0,50	* 27,78 ± 0,62	& # 25,24 ± 0,89
Lateral n.	27,75 ± 0,50	* 23,53 ± 0,62	# 21,92 ±1,02
Thalamus			
Anterodorsal thalamus	49,88 ± 2,00	* 39,05 ± 0,88	# 38,25 ± 1,95
Anteromedial thalamus	31,37 ± 1,11	26,11 ± 1,36	# 25,11 ± 2,13
Anteroventral thalamus	41,72 ± 1,73	* 32,70 ± 1,52	# 34,37 ± 1,27
Mammillary nuclei			
Supramammillary n.	31,20 ± 0,71	* 25,52 ± 1,01	& # 21,96 ± 1,09
Medial medial mamm. n.	30,39 ± 1,68	* 24,42 ± 0,52	# 25,13 ± 1,77
Medial lateral mamm. n.	29,82 ± 0,77	* 23,69 ± 0,50	# 25,37 ± 0,82
Ventral Tegmental area	22,67 ± 1,06	19,57 ± 1,18	18,85 ± 1,19

*: Significant differences between C and BC group (p<0.05). #: Significant differences between C and BC+PBM group (p<0.05). &: Significant differences between BC and BC+PBM group. Mamm=mammillary; n=nucleus; C=control group; BC=behavioural control group; BC+PBM=behavioural photobiomodulation control group.

4. Discussion

The present study aimed to evaluate the effects of PBM in a functionally active neural rat brain network during the execution of a reversal test. We found that after five days of PBM there was a reduction of CCO activity in some limbic regions that are involved in the execution of the reversal task (MS, ENT, CA1, CA3, CeA and SuM), along with higher levels in AccC.

Moreover, we also assessed the effect of this technique in control rats, without learning, and we found a decrease on the oxidative metabolic activity in striatum, medial septum, ENT, hippocampus, amygdala, thalamus nuclei, mammillary nuclei and VTA. Despite applying PBM on the first third of the head, this technique might show a systemic effect causing changes in CCO levels in remote regions through the transmission of its effect in the brain networks.

PBM uses near-infrared light to stimulate, heal and even regenerate damaged tissues and several physiological processes [6,32]. Studies have demonstrated that PBM can reverse apoptotic processes, promote the survival and longevity of the brain cells, leading to brain neuroprotection, and also stimulate angiogenesis [3,10]. It has also displayed photoaging effects and anti-tumor actions through the inhibition of cancer cell proliferation [3]. This breadth of changes is possible due to the absorption of the photons by the CCO which increases ATP levels and leads to numerous biological modifications [33]. However, it should be noted that all these results are dependent on the dose of light fluence applied, being between 600 and 1,200 nm, the higher range of penetration and absorption by the CCO [34].

PBM has been used not only as a treatment of several pathological conditions but also it has been applied to healthy subjects with no clinical symptoms to study its basal effects [35]. Therefore, some studies, such as the research carried out by Wang et al. [36] and Zomorrodi et al. [37], have found that after the application of PBM in human population there is a rise of alpha, beta and gamma frequencies and a reduction of delta and theta frequencies of several brain networks, exhibiting a modulator effect of PBM on brain waves. Some studies have shown that theta rhythm is critical for hippocampal functions and the alteration of these oscillations could impair spatial and nonspatial memory and learning [38,39]. Therefore, several research lines have been focused on PBM's consequential effects during the execution of different tasks and they have found cognitive enhancements. Hence, PBM has reported improvements in human executive and mnesic functions, in learning and attentional capacity [40–42]. Animal research has yielded similar results regarding improving memory and spatial performance and halting cognitive decline [43,44].

In our study, in experiment 1, we examined the effects of five days of 1,064nm PBM on the oxidative metabolic activity of basal control healthy rats. Results showed that, in contrast with the rats that did not receive the PBM treatment, the C+PBM group showed fewer levels of CCO in the striatum, medial septum, ENT, hippocampus, amygdala, thalamus nuclei, mammillary nuclei and VTA. Hence, according to other studies, PBM generated changes in the brain activity of healthy subjects. However, in experiment 2, we assessed the changes in CCO activity after the use of PBM in animals whose known brain networks have been activated by performing a memory task. CCO changes reflect modifications in neural metabolic activity because of learning processes [18]. It has been shown that after this learning there is a reduction in metabolic costs, increasing the efficiency of the areas involved in the task [21]. Furthermore, such pattern of reduction in brain activity has been also related to the difficulty of the task [17]. Similarly, we found that the BC+PBM group displayed lower CCO levels in several limbic areas that were involved in the execution of the memory tasks: MS, ENT, CA1, CA3, CeA, and SuM and higher levels in AccC in comparison with BC group. Therefore, hippocampal regions (CA1, CA3 and ENT) are strongly required for spatial learning [45,46] and they are connected with the SuM, via fornix [47]. The hippocampus also sends and receives afferences from the MS, structure that also send projections to the SuM, generating an active spatial network [46,47]. Conversely, we also found a reduction in the metabolic activity of the amygdala. This region could be linked to the emotional aspects of the task and the lower levels could display fewer levels of stress or anxiety in BC+PBM group [20]. So, the use of PBM could have made easier the execution of the task and could have decreased the metabolic activity of BC+PBM group enhancing the efficiency of this brain active network involved in the spatial memory task. Equivalent results were found by Méndez-López et al. [17]: they showed that there was a CCO activity reduction in several regions involved in a memory task along with, a behavioural improvement when the animals were submitted to only one more trial of this memory task. These results support the idea that an easier execution of the task could be related to the brain changes. Although the animals performed a reversal task that had high difficulty, they were submitted to eight trials after the transfer trial. The large number of trials was enough training to

perform the task correctly and such overtraining could explain why we did not observe behavioural differences between groups that obviously display the effect of PBM in brain active networks. Finally, in BC+PBM group we found a rise of CCO activity in AccC. This area is related to relief learning, the induction of positive emotional states due to the association of a neutral stimulus with the cessation of an aversive event [46,48]. Higher levels of CCO in this area could demonstrate that the BC+PBM group were attributing greater levels of reinforcement to the hidden platform and this could be increasing their seeking behaviours. These brain metabolic changes found by the use of PBM, might explain the marginal difference found in the behavioural tasks because, despite the accurate execution of both groups in the reference memory and reversal task, BC+PBM group displayed a significant latency reduction between day 1 and 4 while BC group remained invariable during all days.

Finally, considering these results, we compared the oxidative metabolic activity of C, BC and BC+PBM groups. Results showed that there was a similar pattern of CCO reduction in BC group compared with C group in several limbic areas: prefrontal regions, striatum, CA1, amygdala, AD, AV and mammillary nuclei. Similarly, BC+PBM group also displayed lower levels of CCO compared with C group but in this case, we found a different pattern of CCO reductions that involve a larger number of limbic regions: prefrontal regions, STD, AccSh, septum, ENT, hippocampus, amygdala, thalamus and mammillary nuclei. As described above, all these regions are distinctly involved in spatial memory, therefore, groups that performed and learned the behavioural tasks showed fewer levels of CCO. Moreover, the BC+PBM group displayed more differences with C group than BC group, showing that PBM prompts changes in many regions involved in the task, making them more efficient and reducing the metabolic cost. Lastly, we found that BC+PBM displayed less CCO levels in MS, ENT, CA1, CA3, BLA and SuM than BC group. This confirm our hypothesis with regards to the effects of PBM on active networks: PBM made the task easier and decreased metabolic activity in the limbic system that was active in the execution of the spatial memory task. In further research, it could be also useful to examine the effects of this technique during the execution of other behavioural tests

that entails other types of learning to elucidate the effects of PBM in diverse active brain networks.

5. Conclusions

The results of the present study show the effects of PBM on brain networks of healthy control rats and on brain networks that were active during the execution of a reversal memory task. Oxidative metabolic activity was evaluated using CCO histochemistry and showed that control rats that received PBM therapy showed less CCO levels in the striatum, medial septum, ENT, hippocampus, amygdala, thalamus nuclei, mammillary nuclei and VTA. Conversely, the administration of PBM in rats that performed a reversal memory task, resulted in lower levels of CCO in several limbic areas that were involved in the execution of the task (MS, ENT, CA1, CA3, CeA, and SuM) and higher levels in AccC, along with a slight difference in scape latencies. These results could show the differential effect of PBM on active brain networks but further studies are necessary to elucidate its effects in different brain networks that are involved in the execution of other memory tasks.

Acknowledgements

We thank AINDACE Foundation (Ayuda a la Investigación del Daño y Enfermedades Cerebrales).

Financial Support

This work was supported by Projects Grants of the MINECO (Ministerio de Economía y Competitividad del Gobierno de España) PSI2017-83893-R, PSI2017-90806-REDT, and MCIU-19-PRE2018-086220 to A.G.M.

Conflict of Interest

The authors declare that they have no conflict of interest to disclose.

References

[1] F. Salehpour, S. Gholipour-Khalili, F. Farajdokht, F. Kamari, T. Walski, M.R. Hamblin,

J.O. DiDuro, P. Cassano, Therapeutic potential of intranasal photobiomodulation therapy for neurological and neuropsychiatric disorders: a narrative review, Rev. Neurosci. 31 (2019) 269–286. https://doi.org/10.1515/revneuro-2019-0063.

[2] R. Meynaghizadeh-Zargar, S. Sadigh-Eteghad, G. Mohaddes, F. Salehpour, S.H. Rasta, Effects of transcranial photobiomodulation and methylene blue on biochemical and behavioral profiles in mice stress model, Lasers Med. Sci. (2019). https://doi.org/10.1007/s10103-019-02851-z.

[3] R.A. Mussttaf, D.F.L. Jenkins, A.N. Jha, Assessing the impact of low level laser therapy (LLLT) on biological systems: a review, Int. J. Radiat. Biol. 95 (2019) 120–143. https://doi.org/10.1080/09553002.2019.1524944.

[4] M. De Oliveira, C.P. Soares, Transcranial Photobiomodulation in The Treatment of Major Depression Abstract, Clin. Psychiatry. (2019) 1–5. https://doi.org/10.21767/2471-9854.100057.

[5] S.M.V. Prasad, T.R. Prasanna, V. Kumaran, N. Venkatachalam, M. Ramees, E.A. Abraham, Low-level laser therapy: A noninvasive method of relieving postactivation orthodontic pain-a randomized controlled clinical trial, J. Pharm. Bioallied Sci. (2019). https://doi.org/10.4103/jpbs.JPBS_303_18.

[6] F. Salehpour, M.R. Hamblin, Photobiomodulation for Parkinson's disease in animal models: A systematic review, Biomolecules. 10 (2020) 1–19. https://doi.org/10.3390/biom10040610.

[7] M.R. Hamblin, Mechanisms and applications of the anti-inflammatory effects of photobiomodulation, AIMS Biophys. 4 (2017) 337–361. https://doi.org/10.3934/biophy.2017.3.337.

[8] M. Hamblin, H. Abrahamse, Factors Affecting Photodynamic Therapy and Anti-Tumor Immune Response., Anticancer. Agents Med. Chem. 20 (2020).

https://doi.org/10.2174/1871520620666200318101037.

[9] G. Litscher, Brain Photobiomodulation—Preliminary Results from Regional Cerebral Oximetry and Thermal Imaging, Medicines. 6 (2019) 11. https://doi.org/10.3390/medicines6010011.

[10] M.R. Hamblin, Mechanisms of photobiomodulation in the brain, in: Photobiomodulation in the Brain, Elsevier, 2019: pp. 97–110. https://doi.org/10.1016/B978-0-12-815305-5.00008-7.

[11] F. Salehpour, J. Mahmoudi, F. Kamari, S. Sadigh-Eteghad, S.H. Rasta, M.R. Hamblin, Brain Photobiomodulation Therapy: a Narrative Review, Mol. Neurobiol. 55 (2018) 6601–6636. https://doi.org/10.1007/s12035-017-0852-4.

[12] L. Lim, M.R. Hamblin, Can the Vielight X-Plus be a Therapeutic Intervention for COVID-19 Infection ?, (2020) 1–13.

[13] H.H. Buzzá, A.C. Zangirolami, C. Kurachi, S. Vanderlei, Acceleration of Newborn Rats Revelopment with the use of photobiomodulation and the near possibility of application in human premature babies, J. Biophotonics. (2019). https://doi.org/doi.org/10.1002/jbio.201800461.

[14] Y. Yang, Y. Zong, Q. Sun, Y. Jia, R. Zhao, White light emitting diode suppresses proliferation and induces apoptosis in hippocampal neuron cells through mitochondrial cytochrome c oxydase-mediated IGF-1 and TNF-α pathways, Free Radic. Biol. Med. 113 (2017) 413–423. https://doi.org/10.1016/j.freeradbiomed.2017.10.382.

[15] W. Xuan, L. Huang, M.R. Hamblin, Repeated transcranial low-level laser therapy for traumatic brain injury in mice: biphasic dose response and long-term treatment outcome, J. Biophotonics. 9 (2016) 1263–1272. https://doi.org/10.1002/jbio.201500336.

[16] P. Cassano, M.A. Caldieraro, R. Norton, D. Mischoulon, N.H. Trinh, M. Nyer, C. Dording, M.R. Hamblin, B. Campbell, D. V. Iosifescu, Reported Side Effects, Weight

and Blood Pressure, after Repeated Sessions of Transcranial Photobiomodulation, Photobiomodulation, Photomedicine, Laser Surg. 37 (2019) 651–656. https://doi.org/10.1089/photob.2019.4678.

[17] M. Méndez-López, M. Méndez, A. Begega, J.L. Arias, Spatial short-term memory in rats: Effects of learning trials on metabolic activity of limbic structures, Neurosci. Lett. 483 (2010) 32–35. https://doi.org/10.1016/j.neulet.2010.07.054.

[18] J.T. Sakata, D. Crews, F. Gonzalez-Lima, Behavioral correlates of differences in neural metabolic capacity, Brain Res. Rev. 48 (2005) 1–15. https://doi.org/10.1016/j.brainresrev.2004.07.017.

[19] A. Poremba, D. Jones, F. Gonzalez-Lima, Functional Mapping of Learning-Related Metabolic Activity with Quantitative Cytochrome Oxidase Histochemistry, in: Cytochrome Oxidase Neuronal Metab. Alzheimer's Dis., 1998: pp. 109–144. https://doi.org/10.1007/978-1-4757-9936-1_4.

[20] N.M. Conejo, H. González-Pardo, F. Gonzalez-Lima, J.L. Arias, Spatial learning of the water maze: Progression of brain circuits mapped with cytochrome oxidase histochemistry, Neurobiol. Learn. Mem. 93 (2010) 362–371. https://doi.org/10.1016/j.nlm.2009.12.002.

[21] M. Méndez-López, M. Méndez, L. López, J.L. Arias, Spatial working memory learning in young male and female rats: Involvement of different limbic system regions revealed by cytochrome oxidase activity, Neurosci. Res. 65 (2009) 28–34. https://doi.org/10.1016/j.neures.2009.05.001.

[22] I.R. Olson, H. Rao, K.S. Moore, J. Wang, J.A. Detre, G.K. Aguirre, Using perfusion fMRI to measure continuous changes in neural activity with learning, Brain Cogn. 60 (2006) 262–271. https://doi.org/10.1016/j.bandc.2005.11.010.

[23] E.W. Gobel, T.B. Parrish, P.J. Reber, Neural correlates of skill acquisition: Decreased

cortical activity during a serial interception sequence learning task, Neuroimage. 58 (2011) 1150–1157. https://doi.org/10.1016/j.neuroimage.2011.06.090.

[24] H. El Khoury, J. Mitrofanis, L.A. Henderson, Exploring the Effects of Near Infrared Light on Resting and Evoked Brain Activity in Humans Using Magnetic Resonance Imaging, Neuroscience. 422 (2019) 161–171. https://doi.org/10.1016/j.neuroscience.2019.10.037.

[25] C. Fidalgo, N.M. Conejo, H. González-Pardo, J.L. Arias, Cortico-limbic-striatal contribution after response and reversal learning: a metabolic mapping study, Brain Res. 1368 (2011) 143–150. https://doi.org/10.1016/j.brainres.2010.10.066.

[26] M. Banqueri, C. Zorzo, A, Gutiérrez-Menéndez, S.G., Higarza, J.L., Arias, M. Méndez, c-Fos and its use in memory research: spatial navigation, in: A. Costa, E. Villalba (Eds), Horizons in Neuroscience Research, Nova Science Publishers, Inc., New York, 2020, pp. 1-54.

[27] V.F. Prado, H. Janickova, M.A. Al-Onaizi, M.A.M. Prado, Cholinergic circuits in cognitive flexibility, Neuroscience. 345 (2017) 130–141. https://doi.org/10.1016/j.neuroscience.2016.09.013.

[28] A. Izquierdo, J.L. Brigman, A.K. Radke, P.H. Rudebeck, A. Holmes, The neural basis of reversal learning: An updated perspective, Neuroscience. 345 (2017) 12–26. https://doi.org/10.1016/j.neuroscience.2016.03.021.

[29] M. Banqueri, J.A. Martínez, M.J. Prieto, S. Cid-Duarte, M. Méndez, J.L. Arias, Photobiomodulation rescues cognitive flexibility in early stressed subjects, Brain Res. (2019) 146300. https://doi.org/10.1016/j.brainres.2019.146300.

[30] F. Gonzalez-Lima, A. Cada, Cytochrome oxidase activity in the auditory system of the mouse: A qualitative and quantitative histochemical study, Neuroscience. 63 (1994) 559–578. https://doi.org/10.1016/0306-4522(94)90550-9.

[31] G. Paxinos, C. Watson, The Rat Brain in Stereotaxic Coordinates Sixth Edition by, 2007.

[32] M.R. Hamblin, S.T. Nelson, J.R. Strahan, Photobiomodulation and Cancer: What Is the Truth?, Photomed. Laser Surg. 36 (2018) 241–245. https://doi.org/10.1089/pho.2017.4401.

[33] A.E. Saltmarche, M.A. Naeser, K.F. Ho, M.R. Hamblin, L. Lim, Significant Improvement in Cognition in Mild to Moderately Severe Dementia Cases Treated with Transcranial Plus Intranasal Photobiomodulation: Case Series Report, Photomed. Laser Surg. 35 (2017) 432–441. https://doi.org/10.1089/pho.2016.4227.

[34] J.D. Carroll, Light sources and dosimetry for the brain and whole body, Elsevier Inc., 2019. https://doi.org/10.1016/b978-0-12-815305-5.00007-5.

[35] M.R. Hamblin, Shining light on the head: Photobiomodulation for brain disorders, BBA Clin. (2016). https://doi.org/10.1016/j.bbacli.2016.09.002.

[36] X. Wang, J. Dmochowski, M. Husain, F. Gonzalez-Lima, H. Liu, Proceedings #18. Transcranial Infrared Brain Stimulation Modulates EEG Alpha Power, Brain Stimul. 10 (2017) e67–e69. https://doi.org/10.1016/j.brs.2017.04.111.

[37] R. Zomorrodi, G. Loheswaran, A. Pushparaj, L. Lim, Pulsed Near Infrared Transcranial and Intranasal Photobiomodulation Significantly Modulates Neural Oscillations: a pilot exploratory study, Sci. Rep. 9 (2019) 1–11. https://doi.org/10.1038/s41598-019-42693-x.

[38] T. Shuman, B. Amendolara, P. Golshani, Theta rhythmopathy as a cause of cognitive disability in TLE, Epilepsy Curr. 17 (2017) 107–111. https://doi.org/10.5698/1535-7511.17.2.107.

[39] M.E. Hasselmo, C.E. Stern, Theta rhythm and the encoding and retrieval of space and time, Neuroimage. 85 (2014) 656–666. https://doi.org/10.1016/j.neuroimage.2013.06.022.

[40] N.J. Blanco, W.T. Maddox, F. Gonzalez-Lima, Improving executive function using

transcranial infrared laser stimulation, J. Neuropsychol. 11 (2017) 14–25. https://doi.org/10.1111/jnp.12074.

[41] F. Gonzalez-Lima, D. Barrett, C. Saucedo, C. Alexander, H. Liu, A. Haley, Transcranial Photobiomodulation in Healthy Subjects: Cognitive Enhancement, Biol. Psychiatry. 85 (2019) S80–S81. https://doi.org/10.1016/j.biopsych.2019.03.208.

[42] A. Jahan, M.A. Nazari, J. Mahmoudi, F. Salehpour, M.M. Salimi, Transcranial near-infrared photobiomodulation could modulate brain electrophysiological features and attentional performance in healthy young adults, Lasers Med. Sci. 34 (2019) 1193–1200. https://doi.org/10.1007/s10103-018-02710-3.

[43] S. Michalikova, A. Ennaceur, R. van Rensburg, P.L. Chazot, Emotional responses and memory performance of middle-aged CD1 mice in a 3D maze: Effects of low infrared light, Neurobiol. Learn. Mem. 89 (2008) 480–488. https://doi.org/10.1016/j.nlm.2007.07.014.

[44] F. Salehpour, F. Farajdokht, M. Erfani, S. Sadigh-Eteghad, S.S. Shotorbani, M.R. Hamblin, P. Karimi, S.H. Rasta, J. Mahmoudi, Transcranial near-infrared photobiomodulation attenuates memory impairment and hippocampal oxidative stress in sleep-deprived mice, Brain Res. 1682 (2018) 36–43. https://doi.org/10.1016/j.brainres.2017.12.040.

[45] N.M. Conejo, H. González-Pardo, G. Vallejo, J.L. Arias, Changes in brain oxidative metabolism induced by water maze training, Neuroscience. 145 (2007) 403–412. https://doi.org/10.1016/j.neuroscience.2006.11.057.

[46] M. Banqueri, M. Méndez, J.L. Arias, Spatial memory-related brain activity in normally reared and different maternal separation models in rats, Physiol. Behav. 181 (2017) 80–85. https://doi.org/10.1016/j.physbeh.2017.09.007.

[47] J.P. Aggleton, S.M. O'Mara, S.D. Vann, N.F. Wright, M. Tsanov, J.T. Erichsen,

Hippocampal-anterior thalamic pathways for memory: Uncovering a network of direct and indirect actions, Eur. J. Neurosci. 31 (2010) 2292–2307. https://doi.org/10.1111/j.1460-9568.2010.07251.x.

[48] J.R. Bergado Acosta, E. Kahl, G. Kogias, T.C. Uzuneser, M. Fendt, Relief learning requires a coincident activation of dopamine D1 and NMDA receptors within the nucleus accumbens, Neuropharmacology. 114 (2017) 58–66. https://doi.org/10.1016/j.neuropharm.2016.11.022.